Structural Engineering and Mechanics, Vol. 11, No. 2 (2001) 211-219
DOI: http://dx.doi.org/10.12989/sem.2001.11.2.211

Folding analysis of reversal arch by the tangent stiffness method

Shin-ichi Iguchi† and Shigeo Goto‡

FORUMEIGHT Ltd., 1-31 Tenya-machi, Hakata-ku Fukuoka, Japan

Katsushi Ijima‡† and Hiroyuki Obiya‡‡

Department of Civil Engineering, Saga University, 1 Honjou Saga, Japan

Abstract. This paper presents the tangent stiffness method for 3-D geometrically nonlinear folding analysis of a reversal arch. Experimental tests are conducted to verify the numerical analysis. The tangent stiffness method can accurately evaluate the geometrical nonlinearity due to the element translating as a rigid body, and the method can exactly handle the large rotation of the element in space. The arch in the experiment is made from a thin flat bar, and it is found that the folding process of the arch may be captured exactly by the numerical analysis with a model consisting of only 18 elements with the same properties.

Key words: large displacement analysis; geometrical nonlinearity; finite rotation; folding experiment.

1. Introduction

This paper presents the tangent stiffness method for the folding analysis of a reversal arch. The proposed method, an extension of the displacement method, does not use nonlinear stiffness equations but a simple iterative method. The iterative process has the same convergence as the Newton-Raphson method. The method distinguishes the nonlinear displacement of an element as a rigid body from other nonlinearities such as material nonlinearity. The method does not need a special theory in order to consider finite rotations for the formulation of the element stiffness equation of each element.

The finite rotations are included in the displacement as axial vectors and thus cannot be summed algebraically. Even by using a highly accurate theory that introduces highly nonlinear terms in the displacement field, the exact solution cannot be obtained by simply adding the finite rotations. Therefore, the new displacement in the iterative process is obtained by using the coordinate transformation matrix instead of simply summing the increment displacement (Goto, S. *et al.* 1998, and Iguchi *et al*. 1997, 1999).

† Programmer
‡ Technical Advisor
‡† Professor
‡‡ Associate Professor

The method does not use strains expressed by the nodal displacements, such as the Lagrange strain (Goto, Y. *et al*. 1983), but by the element deformations defined by setting the element coordinates (Goto, S. *et al*. 1991). The element coordinates are to support the element by a statically determinate condition. The concept in the method is similar to the slope-deflection method. Therefore, the element deformations in a line member become the elongation and the slope deflections at both edges. From elementary statics of structures, the relationship between the element deformations and the element edge forces is straightforward. The application of Pythagoras' theorem allows the exact determination of the elongation, and the geometry of the finite rotation expresses exactly the slope deflection without using the strain tensor.

Though there are many papers published on geometrically nonlinear analysis (Goto, Y. *et al*. 1991, 1996, and Pai and Plazotto 1996a, 1996b), there are relatively few papers furnishing experimental results on large displacement phenomena that verify these theories. The experiment conducted in this study involves folding a reversal arch by giving a torque at an edge. In the experiment, the torque at the fixed edge, and the bending moment and the displacement at the crown were measured. The model in the analysis is composed of 18 elements with the same properties as those of the bar in the experiment. The comparison between the experimental and analytical results shows that the proposed method can accommodate geometrical nonlinearity accurately without dividing the model into very small elements.

2. Tangent stiffness method

The tangent stiffness equation is simply and clearly derived by considering the equilibrium relation given by

$$\boldsymbol{D}=\boldsymbol{JS} \tag{1}$$

The differential of Eq. (1) is given by

$$\delta\boldsymbol{D}=\boldsymbol{J}\delta\boldsymbol{S}+\delta\boldsymbol{JS} \tag{2}$$

$$\delta\boldsymbol{D}=[\boldsymbol{K}_0+\boldsymbol{K}_G]\delta\boldsymbol{d}=\boldsymbol{K}_T(\boldsymbol{JS})\delta\boldsymbol{d} \tag{3}$$

where

$\boldsymbol{D}$, $\boldsymbol{d}$: external force vector and displacement vector
$\boldsymbol{J}$: coordinate transformation matrix from element coordinate to global coordinate
$\boldsymbol{S}$: element edge force vector
$\boldsymbol{K}_0=\boldsymbol{JkJ}^T$: stiffness related to the element stiffness
$\boldsymbol{k}$: element stiffness matrix
$\boldsymbol{K_T}$: tangent stiffness matrix
$\boldsymbol{K}_G=\dfrac{\partial(\delta\boldsymbol{JS})^T}{\partial\delta\boldsymbol{d}}$: geometrical stiffness matrix

The tangent stiffness equation of the method is derived from the differential of the equilibrium equation. Eq. (3) shows that the method can clearly divide the tangent stiffness into the stiffness related to the element stiffness and the stiffness related to the changing of the direction of the element edge force. Thus, the element stiffness and the element edge forces make up the tangent

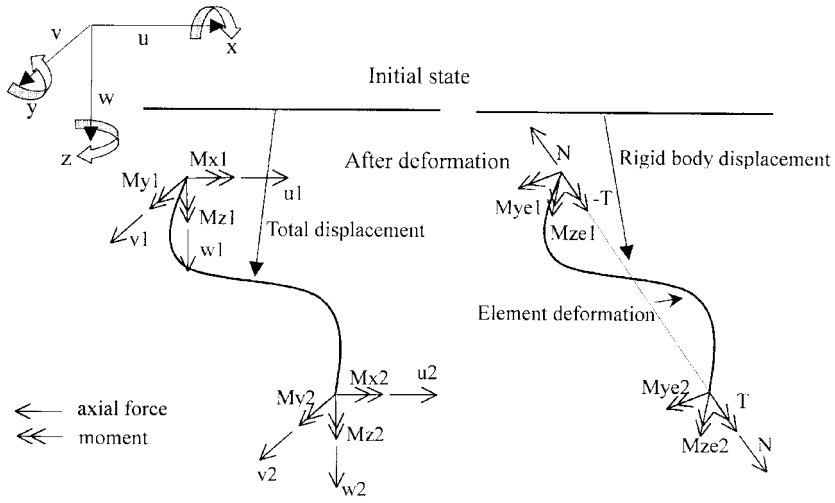

Fig. 1 Definition of element coordinate system and variables

stiffness matrix, and the displacement does not appear in the tangent stiffness matrix.

3. Element coordinates

The right diagram in Fig. 1 shows the element coordinates defined in this method, while the left one shows the nodal forces in the global coordinate system. In the element coordinates, the element has the same support condition as a simple beam, and the element edge forces are independent of each other. The element deformation is complementary to the element edge forces in the work term. More specifically, the elongation is the counterpart of N as derived from Pythagoras' theorem. The slope deflections are the counterparts of the edge moments at both edges, which can be derived from the geometry of finite rotation. This allows the evaluation of the exact displacements of the element as a rigid body, which is crucial for obtaining the solution to large displacement phenomena, such as arch folding.

4. Managing finite rotations

For the updated displacement in the iterative process, the nodal translation can be expressed by the polar vector. Then,

$$\Delta \boldsymbol{u}^{r+1} = \Delta \boldsymbol{u}^{r} + \delta \boldsymbol{u}^{r} \tag{4}$$

On the other hand, since the nodal rotation is the axial vector, the updated rotation is,

$$\Delta \boldsymbol{x}^{r+1} = \Delta \boldsymbol{x}^{r} \oplus \delta \boldsymbol{x}^{r} = \Phi^{-1}\{\Phi(\delta \boldsymbol{x}^{r})\Phi(\Delta \boldsymbol{x}^{r})\} \tag{5}$$

where

r : iterative indicator

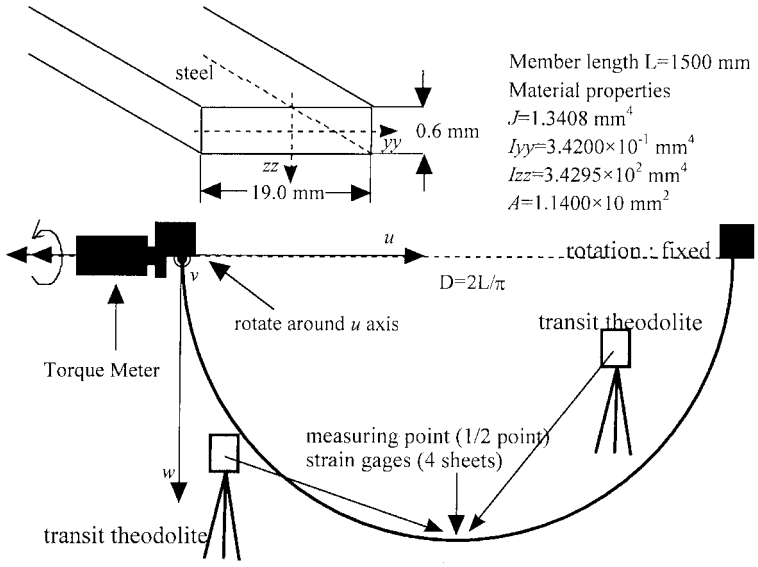

Fig. 2 Outline of experiment

$\Delta \boldsymbol{u}^r$, $\delta \boldsymbol{u}^r$: nodal translation vector and its increment
$\Delta \boldsymbol{x}^r$, $\delta \boldsymbol{x}^r$: nodal rotational vector and its increment

The matrix $\Phi(\boldsymbol{x})$ is shown in Eq. (6) below. When a position vector is multiplied by the matrix, the product is the position vector after rotating around the axial vector $\boldsymbol{x}$. The matrix can express the finite rotation exactly. The first order in the power series of the matrix by the rotation vector $\boldsymbol{x}$ agrees with the transformation matrix derived by Oran (1973). The new rotation in the iterative process is given by the reversal transformation after multiplying the two transformation matrices together, which correspond to the nodal rotation vector and its increment.

$$\Phi(\boldsymbol{x})=\frac{\boldsymbol{x}\boldsymbol{x}^T}{x^2}(1-\cos x)+\boldsymbol{e}\cos x-\frac{\boldsymbol{x}}{x}\times\boldsymbol{e}\ \sin x \tag{6}$$

where $x^2=\boldsymbol{x}^T\boldsymbol{x}$, $\boldsymbol{e}$ is a 3×3 unit matrix and × is the vector product sign.

5. Reversal arch folding

5.1 Experiment

Fig. 2 shows the outline of the experiment, the details of the cross section of the steel member and the primary state of the reversal arch. The primary shape is a state of buckling from the flat bar of steel, so that the arch already has the bending moment. One end is fixed at the post, and the other end is rotated around the u-axis. The rotation angle is 2π from the primary state. As a result of the rotation, the shape changes from the reversal arch to a ring of one and a half revolutions. Fig. 3 shows the folding process. The stress in the member is within the elastic state, while the deformation of the reversal arch is very large. When the rotation at the end reaches 5.934 radians,

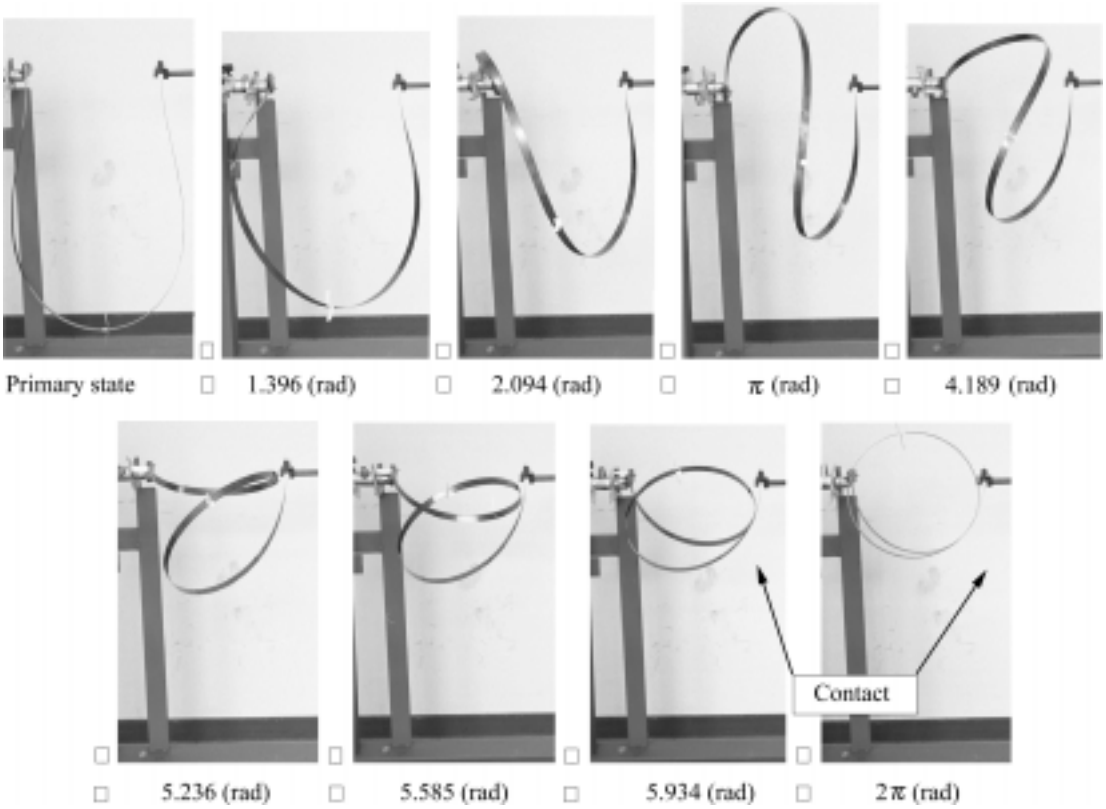

Fig. 3 Experimental results of folding process

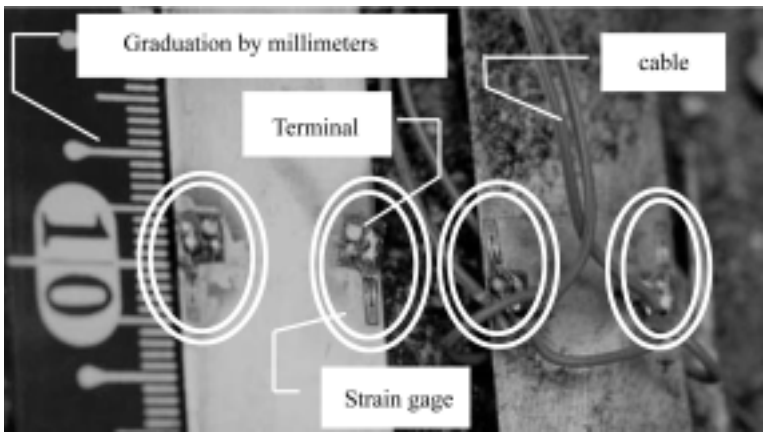

Fig. 4 Strain gages, terminals and codes

two points in the member touch each other. However, the present analysis does not consider the contact forces.

The torque given at one end was measured during the deformation of the arch. Simultaneously, the bending moment was measured using four strain gages, and the displacement by the transit

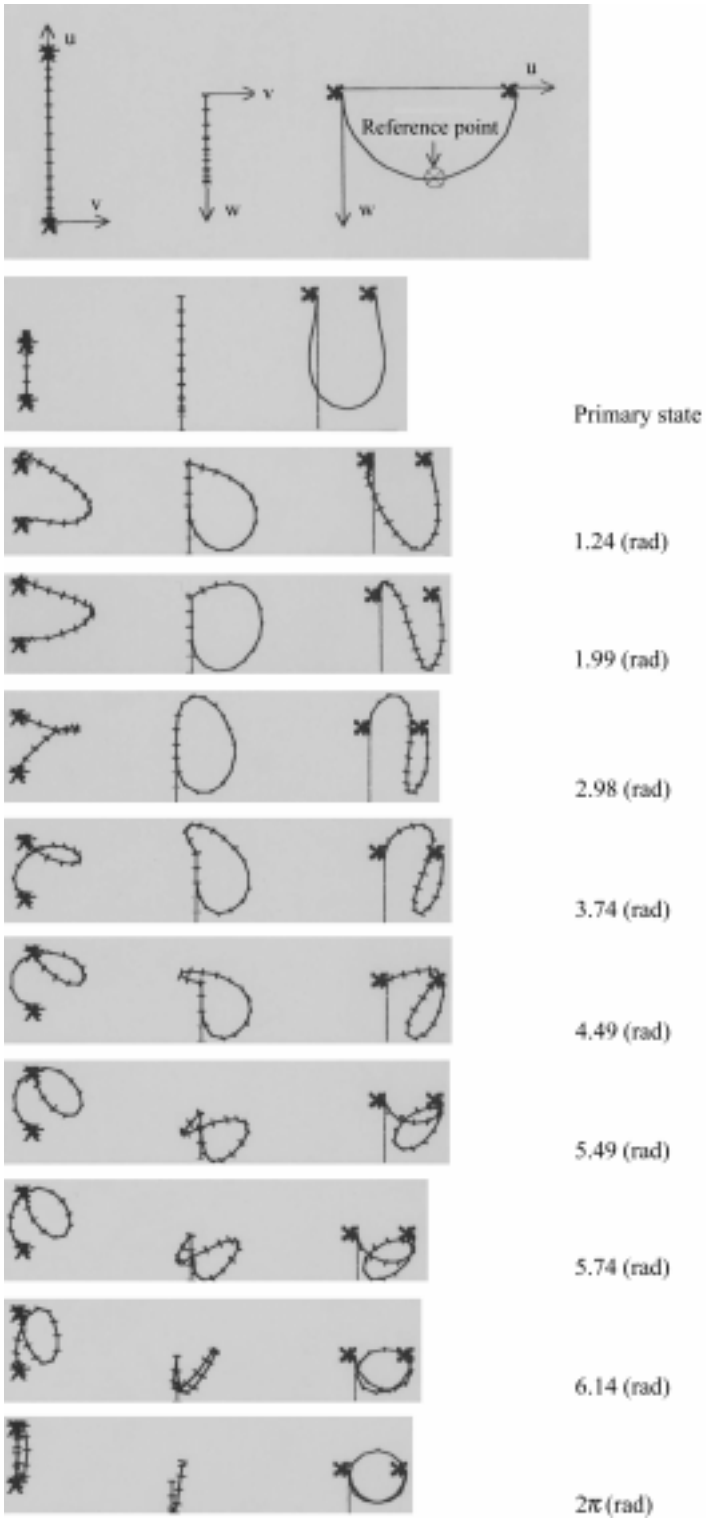

Fig. 5 Analysis of folding process

theodolite. Fig. 4 shows how the bending moments on the experimental model were measured. The experiment was conducted several times, and the measured bending moment values were found to scatter slightly because of dangling of the codes from the strain gages. The deformation is, however, stable during the process.

5.2 Analysis

Fig. 5 shows the analytical model that was used to simulate the experiment and the shapes in the folding process. The model in the analysis is composed of 18 elements with the same properties as the bar in the experiment. The rotational state at each node can be found from the short segments at right angle to the real members in Fig. 5. The analysis is carried out beginning from the half arch with its primary bending stress and dead load. When one end of the arch is displaced 2/3 of the diameter in the $-u$ direction, the arch is deformed to the primary state of the experiment. Then the other end is rotated around the u axis. As shown in Fig. 3, the dead load affects the deformation. The influence of the dead load becomes evident in the solution for the rotation of 2π radians.

The analysis defines the element forces as forces which act at both ends of the element, and they are independent of each other. The element forces and the element deformations make a pair in the work term. The analysis assumes that the relationship between the element forces and the element deformations is linear. Therefore, the nonlinear effect appears only in the translation of the elements as a rigid body.

5.3 Results and discussion

Figs. 6 to 8 show the comparison of the results obtained from the experiment and the numerical analysis. Fig. 6 shows the relationship between the rotation and the torque at the one end. The experimental values are slightly scattered because of dangling of the cables connected to the strain gages and/or rattling of the torque meter. However, the results from the numerical analysis are in good agreement with the experimental results. When the angle of rotation is over 1.33 radians, the torque decreases rapidly. This is why the torque becomes the bending moment in the process of deforming to the ring shape. The reason for the torque remaining after folding is that the ring is not

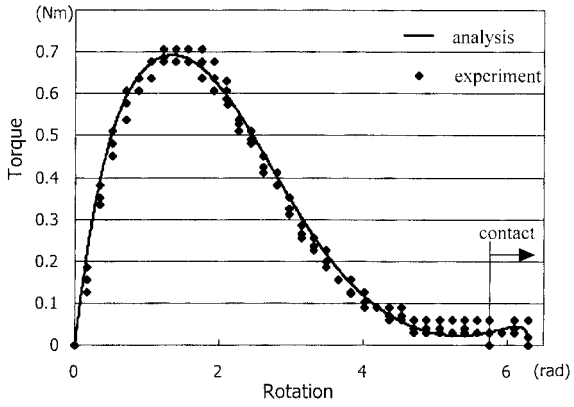

Fig. 6 Rotation vs torque at the end of bar

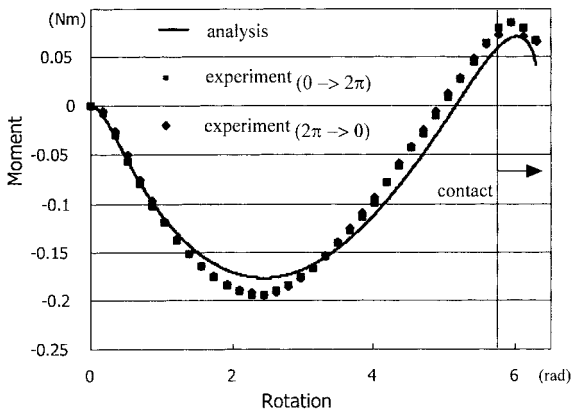

Fig. 7 Bending moment at the crown of arch

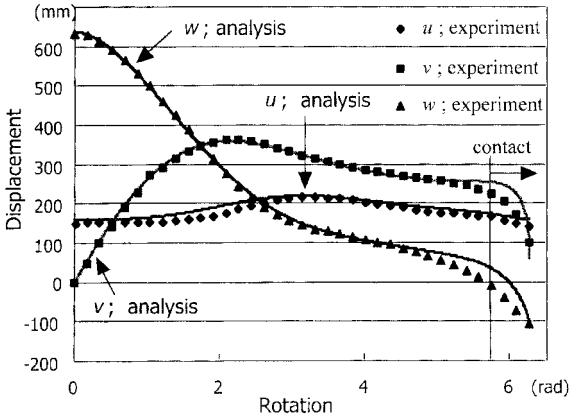

Fig. 8 Displacement at the crown of arch

folded perfectly by the dead load.

Fig. 7 shows the moment at the crown of the reversal arch in the deformation process. There are small differences between the analysis and the experiment. The experimental values may have errors because the actual stiffness was not used in the analysis. Instead, a Young's modulus of 205.8 Gpa was assumed for the steel. Fig. 7 shows the experimental values corresponding to the rotation angle at the edge from 0 radian to 2π radians and also in the reverse manner from 2π radians to 0 radian. The final state coincides with the primary state, and the bending moment at the final state becomes zero. Therefore, the elastic state of the material was maintained during the experiment.

Fig. 8 shows the displacement at the crown of the arch. Except for the case after contact of the bar, the numerical analysis agrees well with the experiment during the process of the deformation. In addition, the shapes of the deformation coincide with the shapes obtained in the experiment.

These figures show that the model composed of only 18 elements in the analysis can simulate the experiment very well. Furthermore, by assuming just linear material behaviour, the analysis can simulate the large displacement phenomena with finite rotation.

6. Conclusions

The paper shows that the tangent stiffness method may be used to handle finite rotation in the folding analysis of a reversal arch. In addition, the definition of the element coordinate system is essential for evaluating the element deformation in an exact manner. Even if the increment of rotation is very small, the rotation must be computed as an axial vector. One method for computing the rotation is to use the coordinate transformation matrix.

The analysis, which considers the finite rotation exactly, can simulate large displacement phenomena of frame structures in space without the need to divide the structure into very fine elements. If the strains in the structure are within the elastic regime, the analysis does not need to consider the geometrical nonlinearity in the element.

Large deformation experiments with the model described in this paper have been achieved. These have never been done before. The measured torque at the end of arch and the moment and the

displacement at the crown obtained in the experiments are sufficient for comparison with the analytical results. However, there is still room for improvement in the measurement technique.

References

Goto, S., Aramaki, G. and Ijima, K. (1991), "A study on tangent geometric stiffness without including inherent stiffness of element itself ", *Journal of Structural Engineering*, **37A**, 315-328 (in Japanese).

Goto, S., Ijima, K., Obiya, H. and Iguchi S. (1998), "Integrating methods of finite rotation and convergence of solutions for 3-D large deformational analysis", *Proceedings of the Conference on Computational Engineering and Science*, **3**, 757-760 (in Japanese).

Goto, Y., Hasegawa, A. and Nishino, F. (1983), "Accuracy of finite displacement analysis of plane flames", *Proc. of JSCE*, **331**, 33-44 (in Japanese).

Goto, Y., Watanabe, Y., Kasugai, T. and Matuura, S. (1991), "Deployable rings utilizing an elastic buckling phenomenon accompanying finite rotation in space", *Proc. of JSCE*, **428**, 117-125 (in Japanese)

Goto, Y., Watanabe, Y., Kasugai, T. and Obata, M. (1996), "Letter to the Editor", *Int. J Solid Structures*, **33**(9), 1369-1370.

Iguchi, S., Goto, S., Ijima, K. and Obiya, H. (1997), "Large deformation analysis of spatial folding by the tangent stiffness method", *Proc. of ICCCBE*, **1**, 209-214.

Iguchi, S., Goto, S., Ijima, K. and Obiya, H. (1999), "A study on folding problems of polygonal ring", *Journal of Structural Engineering*, **45A**, 311-319 (in Japanese).

Oran C. (1973), "Tangent stiffness in space frames", *Journal of the Structural Division*, ASCE, **99**(ST6), 987-1001.

Pai, P.F. and Plazotto, A.N. (1996a), "Large deformation analysis of flexible beams", *Int. J. Solids Structures*, **33**(9), 1335-1353.

Pai, P.F. and Plazotto, A.N. (1996b), "Authors' Closure", *Int. J. Solids Structures*, **33**(9), 1371-1373.